Cellular and Metabolic Engineering **Biotechnology and Bioengineering**

DOI 10.1002/bit.26407

Dynamic Monitoring of p53 Translocation to Mitochondria for the Analysis of Specific Inhibitors Using Luciferase-fragment Complementation†

Running title: Dynamic monitoring of p53 translocation

Natsumi Noda[1], Raheela Awais[2], Robert Sutton[3], Muhammad Awais[3]*, and Takeaki Ozawa[1]*

[1]Department of Chemistry, School of Science, The University of Tokyo, 7-3-1 Hongo, Bunkyo-ku, Tokyo 113-0033, Japan

[2]School of Life Sciences, Crown Street, University of Liverpool, United Kingdom

[3]NIHR Liverpool Pancreas Biomedical Research Unit, Institute of Translational Medicine, University of Liverpool, Royal Liverpool University Hospital, Daulby Street, Liverpool L7 8XP, United Kingdom

*Correspondence should be addressed to
M. A. and T. O.
Email (M. A.): awais@liverpool.ac.uk
Phone: +44 151 706 4279
Email (T. O.): ozawa@chem.s.u-tokyo.ac.jp
Phone: +81 3 5841 4351
Fax: +81 3 5802 2989

†This article has been accepted for publication and undergone full peer review but has not been through the copyediting, typesetting, pagination and proofreading process, which may lead to differences between this version and the Version of Record. Please cite this article as doi: [10.1002/bit.26407]

Additional Supporting Information may be found in the online version of this article.

Received June 23, 2017; Revision Received August 14, 2017; Accepted August 17, 2017

ABSTRACT

Intracellular protein translocation plays a pivotal role in regulating complex biological processes, including cell death. The tumor suppressor p53 is a transcription factor activated by DNA damage and oxidative stress that also translocates from the cytosol into the mitochondrial matrix to facilitate necrotic cell death. However, specific inhibitors of p53 mitochondrial translocation are largely unknown. To explore the inhibitors of p53, we developed a bioluminescent probe to monitor p53 translocation from cytosol to mitochondria using luciferase fragment complementation assays. The probe is composed of a novel pair of luciferase fragments, the N-terminus of green click beetle luciferase CBG68 (CBGN) and multiple-complement luciferase fragment (McLuc1). The combination of luciferase fragments showed significant luminescence intensity and high signal-to-background ratio. When the p53 connected with McLuc1 translocates from cytosol into mitochondrial matrix, CBGN in mitochondrial matrix enables to complement with McLuc1, resulting in the restoration of the luminescence. The luminescence intensity was significantly increased under hydrogen peroxide-induced oxidative stress following the complementation of CBGN and McLuc1. Pifithrin-μ, a selective inhibitor of p53 mitochondrial translocation, prevented the mitochondrial translocation of the p53 probe in a concentration-dependent manner. Furthermore, the high luminescence intensity made it easier to visualize the p53 translocation at a single cell level under a bioluminescence microscope. This p53 mitochondrial translocation assay is a new tool for high-throughput screening to identify novel p53 inhibitors, which could be developed as drugs to treat diseases in which necrotic cell death is a major contributor.

Keywords: p53 translocation, luciferase-fragment complementation assays, mitochondria

INTRODUCTION

P53 is the guardian of the genome and regulates cellular responses to numerous stresses. It is well characterized and recognized as tumor suppressor, most notably by acting as a transcription factor (Bieging and Attardi 2012; Bieging et al. 2014). Following DNA damage or potent cellular stress, p53 inhibits cellular proliferation and/or induces apoptotic cell death by transactivation of variety of genes, among which are cyclin dependent kinase inhibitor p21 and pro-apoptotic BAX (Bcl-2-associated X protein) or PUMA (p53 upregulated modulator of apoptosis) (Bieging and Attardi 2012; Reinhardt and Schumacher 2012; Vogelstein et al. 2000). In the presence of a low level of stress, p53 elicits DNA repair and antioxidant protein production to restore normal cellular function (Bieging et al. 2014; Levine and Oren 2009; Sablina et al. 2005). In addition to apoptotic and senescence regulation, p53 also controls genes for cellular metabolism (Maddocks and Vousden 2011), immune responses (Menendez et al. 2013), angiogenesis (Teodoro et al. 2006; Zhang et al. 2000), cell differentiation (Tedeschi and Di Giovanni 2009), motility, migration (Roger et al. 2006) and reproduction (Hu et al. 2007). One of the most prominent activities of p53 independent of transcription is to induce cell death by acting on mitochondria in response to stress. There, p53 interacts with the apoptosis regulators of the BCL-2 family and promotes mitochondrial outer membrane (MOM) permeabilization, which triggers apoptosis (Chipuk et al. 2004; Leu et al. 2004; Marchenko and Moll 2014).

Translocation of p53 to the mitochondria is not restricted to the MOM. In response to an oxidative insult p53 penetrates into the mitochondrial matrix and facilitates in opening of the mitochondrial permeability transition pore (MPTP) in the

inner mitochondrial membrane (Dashzeveg and Yoshida 2015; Marchenko and Moll 2014; Vaseva et al. 2012). Persistent opening of the MPTP in response to sustained cytosolic calcium and/or reactive oxygen species elevations initiates necrotic cell death in a broad range of life threatening diseases including ischemia-reperfusion injury of the heart, brain and kidney, acute pancreatitis, muscular dystrophies and neuro-degeneration (Bernardi and Di Lisa 2015; Kwong and Molkentin 2015; Millay et al. 2008; Mukherjee et al. 2016; Vaseva et al. 2012). To avoid necrotic cell death caused by these diseases, inhibitors of p53 mitochondrial translocation are strong candidates for the therapeutic agents.

To explore the inhibitors of p53 mitochondrial translocation using living cells, a method for high-throughput drug screening system is needed. To visualize translocation of a protein into a specific organelle, fluorescent proteins connected with the target are often used. The resolution is sufficient to discriminate the organelle inside the living cells. However, it is not a suitable tool to evaluate the time dependent change of p53 mitochondrial translocation in cell populations because of the probability of fluorescence bleaching by excitation light.

Bioluminescent probes have the advantages of low background, high signal-to-noise ratio and wide dynamic range of signals (Ozawa et al. 2013), potentially applicable to high-throughput drug screening. Bioluminescent probes used in a protein-fragment complementation assay (PCA) may be particularly useful in the analysis of protein-protein interactions, protein localization, detection and the monitoring of the activity of steroid hormones and of second messengers (Wehr and Rossner 2016). To perform high-throughput drug screening using luciferase fragment complementation assays, a pair of luciferase fragments is required that emits a strong

luminescence signal upon complementation. We previously established a pair of luciferase fragments using the N-terminal end of a Brazilian click beetle (Emerald Luc; ELuc) (Nakajima et al. 2010; Viviani et al. 1999) and the C-terminal end of a Caribbean red click beetle luciferase (CBR) with three point mutations (multiple-complement luciferase fragment; McLuc1) (Hida et al. 2009). The usefulness of McLuc1 was demonstrated by the complementation with ELucN, CBRN or the N-terminus of firefly luciferase (FLucN).

In this study, we show a new pair of luciferase fragments using the N-terminus of Caribbean green click beetle luciferase CBG68 (CBGN) for complementation with McLuc1 to achieve enhanced luminescence for a highly sensitive PCA in single living cells. The CBGN-McLuc1 pair was used for monitoring p53 translocation from the cytosol to mitochondria in live cells. Oxidative stress induced mitochondrial translocation of p53, which was detected by restoration of the luminescence signal through the combination of mitochondrially located CBGN with McLuc1 connected to p53. We investigated effects of two distinct inhibitors of p53, pifithrin-μ (PFT-μ) (Strom et al. 2006) and pifithrin-α (PFT-α) (Komarov et al. 1999), on the p53 translocation into mitochondria. The PFT-μ is believed to affect the p53 translocation to mitochondria under oxidative stress. We show direct evidence that mitochondrial translocation of p53 is inhibited by PFT-μ in a concentration-dependent manner. The potential applicability to screening different chemicals using the probe is discussed.

RESULTS

A New Pair of Luciferase Fragments for Highly Sensitive Complementation Assays. We previously developed a pair of bioluminescent probes to assess protein-protein interactions using luciferase fragment of ELucN (1-412 amino acids; aa) together with McLuc1 (395-542 aa). The bioluminescent probes showed a high signal-to-background (S/B) ratio upon protein-protein interactions (Hida et al. 2009). Nevertheless the luminescence intensity of the ELucN-McLuc1 combination was not sufficient for visualizing protein-protein interactions at a single cell level with bioluminescence microscopy. The McLuc1 is originated from CBR with three point mutations, and CBG and CBR are based on a luciferase gene originally cloned from a Caribbean click beetle *Pyrophorus plagiophthalamus*. Therefore, we predicted that the CBGN fragment has a potential to complement to McLuc1 with higher efficiency. To improve the signal sensitivity, we used CBGN (1-413 aa) instead of ELucN to complement with McLuc1 and generated a CBGN_FKBP vector (Figure 1). To compare the luminescence intensities upon complementation, we used rapamycin-induced interaction between FK506-binding protein (FKBP) and FKBP-binding domain (FRB) (Banaszynski et al. 2005; Hida et al. 2009). Human embryonic kidney (HEK) 293T cells were co-transfected with ELucN_FKBP and FRB_McLuc1 or CBGN_FKBP and FRB_McLuc1 vectors. After 2 days incubation, the cells were treated with 1 μM rapamycin or dimethyl sulfoxide (DMSO, control), and the luminescence intensities were measured using a microplate reader (Figure 2). The S/B ratio of the ELucN-McLuc1 compared to CBGN-McLuc1 complementation was similar; however, with CBGN-McLuc1 complementation, rapamycin-treated cells showed an 11-fold increase in luminescence over vehicle control. In addition, the luminescence intensity

from the CBGN-McLuc1 complementation was ~8-fold higher than the ELucN-McLuc1 complementation in rapamycin-treated cells. These results indicate that CBGN-McLuc1 complementation is more efficient and likely to be more useful in bioluminescence PCAs notably for imaging protein-protein interactions in living cells.

Basic Scheme for Monitoring p53 Translocation into Mitochondria with Novel Luciferase-fragment Complementation. We constructed a set of novel probes for monitoring p53 translocation from the cytosol into mitochondria using the new CBGN-McLuc1 complementation pair (Figure 3a). HEK293T cells were co-transfected with MITO_CBGN and p53_McLuc1. The luciferase fragment of CBGN is localized in the mitochondria as a result of MITO (a mitochondrial matrix targeting signal) (Ozawa et al. 2003). Upon H_2O_2 treatment of transfected cells, p53_McLuc1 moves into mitochondria, where McLuc1 complements with CBGN resulting in emission of bioluminescence (Figure 3b).

Luminescence Intensity of CBGN-McLuc1 Complementation Depends on p53 Translocation from the Cytosol into Mitochondria under H_2O_2 Treatment. To confirm whether the p53_McLuc1 probe translocates into mitochondria and emits luminescence in living cells, HEK293T cells were transiently co-transfected with p53_McLuc1 and MITO_CBGN. The transfected cells were treated with different concentrations of H_2O_2 (0.05, 0.1, 0.2 or 0.4 mM) or deionized water (dw, control), and their luminescence intensities measured with a microplate reader (Figure 4a). The intensity of the cells transfected with the MITO_CBGN and p53_McLuc1 started to increase immediately following 0.2 or 0.4 mM H_2O_2 treatment ($p < 0.01$ vs. respective

vehicle control). On the other hand, the intensity of the cells treated with 0.05 and 0.1 mM H_2O_2 started to increase at 15 min and 10 min, respectively ($p < 0.01$ vs. respective vehicle control). This demonstrates an efficient complementation of CBGN-McLuc1 fragments upon p53 translocation into mitochondria. The luminescence intensities were statistically analyzed at every time point and quantified (Figure 4a, right) at 120 min when signal reached a plateau (Figure 4a, left). The luminescence of the cells treated with 0.1-0.4 mM H_2O_2 showed significant increases compared to that of 0.05 mM H_2O_2 (Figure 4a, right). Consequently, dose of 0.1 mM H_2O_2 was used for oxidative stress in the subsequent experiments.

To evaluate the direct effects of H_2O_2 on luciferase activity, full-length CBG luciferase was expressed in mitochondria by transfecting cells with MITO_CBG and stimulated with H_2O_2 under the same experimental conditions. Although no change in luminescence signal was observed in the vehicle control, the luminescence intensity of the cells significantly decreased 129 min after treatment of the cells with 0.1 mM H_2O_2 ($p < 0.05$ vs. vehicle control) (Figure 4b). These results indicate that H_2O_2 in the 0.05-0.4 mM concentration range partly inhibited luciferin-luciferase reaction in HEK293T cells. As the bioluminescence is an ATP-dependent process and ATP is produced by mitochondria, the observed small decrease in luminescence could result from oxidative mitochondrial damage. Therefore, the luminescence intensities can be measured over 120 min after H_2O_2 treatment.

To exclude a possibility that the elevation of the luminescence intensity originated from an increase in the amount of the luciferase probes, we analyzed the protein levels of the cells expressed p53_McLuc1 and MITO_CBGN under the same conditions at 120 min (Figure 4c). No significant change in the protein level was

observed in the presence or absence of H_2O_2. Taken these results together, we conclude that the luminescence signal from the CBGN-McLuc1 complementation originates from p53 translocation from the cytosol into the mitochondrial matrix induced by oxidative stress.

Effect of PFT-μ and PFT-α on the p53 Translocation into Mitochondria. Next, to demonstrate the applicability of the p53 translocation probes for chemical library screening, we investigated the inhibitory effects of known p53 inhibitors on p53 translocation into mitochondria. The cells transfected with p53_McLuc1 and MITO_CBGN were treated with different concentrations of PFT-μ or DMSO for 1 h and then stimulated with H_2O_2. PFT-μ caused a reduction in luminescence intensity in a concentration-dependent manner, with luminescence completely abolished at 40 μM PFT-μ (Figure 5a). When cells expressing full-length CBG68 were exposed to H_2O_2 in the presence of PFT-μ, no significant difference in luminescence was observed regardless of the concentration of PFT-μ (Figure 5b), indicating that PFT-μ did not interfere with the luciferase activity in mitochondria. We also analyzed protein levels of p53_McLuc1 and MITO_CBGN in cells treated with PFT-μ before H_2O_2 exposure and found no difference in protein levels in the presence or absence of PFT-μ (Figure 5c). These results indicate that PFT-μ did not interfere with the reporter functions of luciferase in these cells but rather that PFT-μ inhibits p53 translocation into the mitochondrial matrix, rendering McLuc1 unable to complement with the mitochondrial localized CBGN in HEK293T cells to generate luminescence.

PFT-α inhibits p53 mediated transcriptional activation and apoptosis (Komarov et al. 1999). It is not clear, however, whether PFT-α also inhibits p53 translocation to

mitochondria. Using our probes, we evaluated the effect of PFT-α on p53 translocation into mitochondria in HEK293T cells. Cells transfected with p53_McLuc1 and MITO_CBGN were treated with different concentrations of PFT-α or DMSO for 1 h and exposed to H_2O_2 thereafter. PFT-α, even at 20 μM, was unable to reduce luminescence induced by H_2O_2 (Figure 6a). This indicates that PFT-α does not inhibit p53 translocation from the cytosol into mitochondria. We also examined the effect of PFT-α on the luciferin-luciferase reaction using the full-length CBG luciferase. No significant increase in luminescence intensities was observed regardless of the concentration of PFT-α (Figure 6b). All these results indicate that PFT-α neither interferes with luciferase activity nor inhibits p53 translocation into mitochondria.

Time-lapse Bioluminescence Imaging of p53 Translocation into Mitochondria. For measurement of bioluminescence using a pair of luciferases emitting different wavelengths, filters are set to select a particular wavelength in the microscopic system, based on the bioluminescence spectrum of each luciferase. To enable future use of the CBGN-McLuc1 complemented luciferase with other luciferases, we analyzed the bioluminescence spectrum of the CBGN-McLuc1 complemented luciferase. HEK293T cells were transiently co-transfected with p53_McLuc1 and MITO_CBGN, then the emission spectrum of the cell lysates was determined, exhibiting green light with an emission maximum at 556 nm (Figure 7), unlike CBG68 luciferase that has an emission maximum of 537 nm. The spectral shift at 19 nm may originate from the use of McLuc1, generated from the C-terminus of the CBR with three point mutations.

To temporally monitor p53 translocation into mitochondria using the bioluminescent probe, time-lapse images of cells expressing p53_McLuc1 and

MITO_CBGN were obtained sequentially in the presence or absence of 0.1 mM H_2O_2 at single cell level (Figure 8 and Supporting Video 1, 2). As observed with the microplate reader, the luminescence intensity of the cells significantly increased upon addition of H_2O_2 from 20 min onward under the microscope (Figure 8a, b). On the other hand, the cells treated with vehicle showed no significant difference in luminescence. Although the subcellular localization of the probes was limited by optical resolution and long exposure times, bioluminescence imaging of HEK293T cells transfected with p53_McLuc1 and MITO_CBGN captured translocation of p53 at the single cell level.

DISCUSSION

Protein translocation from one subcellular compartment to another in response to a physiological signal or under stress is a fundamental cellular process required in the regulation of complex biological systems within living organisms. New technologies and functional assays have always been needed to monitor dynamic cellular processes, such as protein translocation and protein-protein interactions, in real-time in the physiological environment of live cells. P53 transcriptional activities affected via the nucleus, such as cell cycle arrest and apoptotic cell death regulation, have been well characterized for many years. Transcriptional independent matrix-based p53 activity for promoting necrotic cell death in response to oxidative stress, however, is relatively a new addition in functional activities of p53 (Marchenko and Moll 2014). The new, improved, bioluminescent protein-fragment complementation pair that we report here allowed real-time assays and imaging of transcriptionally independent activity of p53 in live cells. Unlike techniques used to evaluate p53 translocation phenomena using fixed cells or cell lysates where H_2O_2 treatment is required for 4-6 hours (Guo et al. 2014; Vaseva et al.

2012), p53 translocation can be monitored in our technique as soon as 15 minutes with very low concentration of H_2O_2, because of efficient complementation of the new luciferase fragments. It has been reported that p53 translocation to mitochondria occurs within 10 min after 12-O-tetradecanoylphorbol-13-acetate treatment for oxidative stress (Zhao et al. 2005). Although the stimulus is different from oxidative stress in our system, the result in terms of the time scale was consistent with the previous ones. In radiosensitive organs, thymus and spleen, p53 translocation to mitochondria is detectable at 30 min after γ-irradiation (Erster et al. 2004). Our p53 probe will be applicable to detection of the p53 with more rapid dynamic motion in the organs.

Upon oxidative stress, p53 monoubiquitylated by MDM2 (a p53 ubiquitin E3 ligase) is promoted the translocation to mitochondria (Marchenko et al. 2007). MDM2-mediated p53 monoubiquitylation is mediated by Drp1 (dynamin-related protein 1) (Dashzeveg and Yoshida 2015; Guo et al. 2014). Our p53 probe may contribute to further elucidation of p53 mitochondrial translocation mechanism.

Functional p53 is highly desirable for effective anticancer treatment targeted at the induction of death in tumor cells (Bieging et al. 2014). However, p53 expression in normal tissues and organs makes these vulnerable to damage from anticancer therapy (Chow et al. 2000; Komarova et al. 1997; Song and Lambert 1999). To minimize the side effects of chemo- and radiotherapy on normal tissue, inhibition of p53 mitochondrial translocation or temporary suppression of its transcriptional activity could be useful. The p53 inhibitor PFT-μ is capable of maintaining the mitochondrial integrity and prevents both paclitaxel and cisplatin-induced mechanical allodynia (Krukowski et al. 2015). A single dose of PFT-μ is able to significantly reduce *in vitro* thymocyte death and *in vivo* lethality in mice induced by gamma irradiation (Strom et al.

2006). Inhibition of p53 with PFT-μ has also shown promising results using rat neonatal brain ischemia to model perinatal hypoxia/asphyxia-induced brain damage (Nijboer et al. 2011). Here, we have succeeded in showing direct evidence in live cells that PFT-μ inhibits the translocation of p53 from cytosol into mitochondria under H_2O_2 exposure. Hence, the developed p53 probe allows for exploration of novel inhibitors for mitochondrial translocation of p53. In contrast, p53 transcriptional inhibitor, PFT-α, did not prevent the mitochondrial translocation of the p53 probe under oxidative stress in HEK293T cells. This result is in reasonable agreement with the effects of PFT-α, which blocks p53-dependent transcriptional activation and apoptosis (Komarov et al. 1999). Taken together, the present PCA for monitoring p53 mitochondrial translocation is a novel tool that may be used effectively in live cells for high-throughput screening on the identification of mitochondrial p53 inhibitors, in the search for drugs to prevent or reduce necrotic cell death in a range of acute and chronic diseases as in reducing side effects of anticancer therapies.

There are some available PCA-based tools such as β-lactamase (Remy et al. 2007) and β-galactosidase (Rossi et al. 1997). Since PCAs using β-lactamase and β-galactosidase are performed by use of the fluorescent substrates in living cells, long-term measurement for high-throughput screening is not suited. Moreover, β-galactosidase is high molecular weight (116 kDa) compared to FLuc (61 kDa) and CBG68 (60 kDa). In contrast, NanoLuc (Nluc) was engineered from the deep sea shrimp *Oplophorus gracilirostris* as a small luciferase subunit (19 kDa), which showed an activity greater than that of either firefly or *Renilla* luciferases (Hall et al. 2012). However, a short half-life, within 4 h at 37°C, of Nluc substrate (furimazine, a coelenterazine analog) could limit its applications for long-term monitoring. By contrast,

D-luciferin is a quite stable substrate compared to *Cypridina* luciferin and the luciferins of krill and dinoflagellates (Shimomura 2012). Thus, the luciferases with D-luciferin as a substrate are suitable for high-throughput drug screening.

Finally, we optimized the luciferase fragments to boost overall photon productions. It has been reported that CBG99N (2-413 aa) complemented with CBG99C (395-542 aa), and the CBG99C was used for dual-color luciferase PCAs (Villalobos et al. 2010). CBG99 includes one amino acid difference compared to the amino acids of CBG68. Also, CBG99C does not complement with the FLucN (Villalobos et al. 2010). In contrast, McLuc1 can complement with ELucN, CBRN, FLucN (Hida et al. 2009), or CBGN. Thus, the new pair of CBGN and McLuc1 will be applicable for dual-color luciferase fragment complementation assays for simultaneous detection of proteins in two different compartments of a cell.

CONCLUSION

The new pair of luciferase fragments, CBGN and McLuc1, showed efficient complementation with significant bioluminescence intensity and high S/B ratio, which allowed direct monitoring and visualization of p53 translocation from the cytosol into mitochondrial matrix in living cells subjected to oxidative stress. The assay specificity has been demonstrated by using two distinct p53 inhibitors. The present PCA can serve as a new tool for high-throughput screening on the identification of specific p53 inhibitors for the development of drugs to protect mitochondrial function during the pathogenesis of different diseases.

METHODS

Vector Construction. FKBP binds with FRB in the presence of rapamycin. Previously, we constructed CBRN_FKBP and FRB_McLuc1 vectors to evaluate the complementation of the CBRN-McLuc1 fragments. McLuc1 was developed from the C-terminus of the CBR by introducing three point mutations, F420I, G421A and E453S (Hida et al. 2009). To generate CBGN, the DNA fragment encoding the N-terminus (1-413 aa) of the CBG68 was amplified by PCR using the pCBG68-Basic vector (Promega) as a template. The CBRN in the CBRN_FKBP was replaced with the amplified CBGN to construct the CBGN_FKBP. The CBGN_FKBP and FRB_McLuc1 were used to evaluate the complementation efficiency of the CBGN and McLuc1 fragments.

A hygromycin B resistance gene was amplified by PCR using pQCXIH vector (Takara-Clontech) as a template, and a fragment of FLAG epitope tag was generated by oligonucleotide annealing. Myc epitope and a six-histidine (myc-His), and a neomycin resistance gene in pcDNA3.1/myc-His (B) vector (Thermo Fisher Scientific-Invitrogen) were replaced with the FLAG epitope tag and the hygromycin B resistance gene, respectively (pcDNA3.1_FLAG_Hygro^r vector). The fragment of CBGN and full-length CBG were amplified by PCR, and fragments of a MITO were generated by oligonucleotide annealing. The MITO translocates into the mitochondrial matrix (Ozawa et al. 2003). The MITO and CBGN or full-length CBG were inserted into pcDNA3.1_FLAG_Hygro^r vector. A puromycin resistance gene was amplified by PCR using pLVSIN-CMV pur vector (Takara) as a template, which was replaced with a Zeocin resistance gene in pcDNA4/V5-His (B) vector (Thermo Fisher Scientific-Invitrogen). Human p53 (NCBI reference sequence: NP_000537.3) and

McLuc1 were amplified by PCR using Human Brain, whole QUICK-Clone cDNA (Clontech) and FRB_McLuc1 as templates, respectively. These fragments were inserted into the modified pcDNA4/V5-His (B) vector.

Cell Cultures and Transfection. HEK293T cells were obtained from Abcam and maintained in Dulbecco's modified Eagle's medium (DMEM) supplemented with 10% fetal bovine serum (FBS) and penicillin–streptomycin (100 units/ml and 100 μg/ml, respectively) under 5% CO_2 at 37°C. The constructed vectors were transfected into HEK293T cells using TransIT-LT1 reagent (Takara-Mirus) according to the manufacturer's instructions.

Rapamycin, PFT-μ, or PFT-α Treatment and Luciferase Assay. The luminescence intensities by complementation of CBGN and McLuc1 fragments or ELucN and McLuc1 fragments were evaluated based on FKBP-FRB interactions. ELuc (Toyobo) is a green-emitting luciferase (λ_{max}=538 nm) (Nakajima et al. 2010; Viviani et al. 1999).

HEK293T cells were spread on a 96-well microtiter plate and cultured in DMEM supplemented with 10% FBS and penicillin–streptomycin for 1 day. The cells were transiently co-transfected with CBGN_FKBP and FRB_McLuc1 or ELucN_FKBP and FRB_McLuc1, respectively, for 2 days, and the medium of the cells was replaced with phenol red-free DMEM containing 25 mM HEPES (Thermo Fisher Scientific-Gibco), 1 μM rapamycin (Santa Cruz Biotechnology) or DMSO (vehicle control), and 0.2 mM D-luciferin. Luminescence intensity was measured with a microplate reader, Mithras LB 940 (Berthold technologies), at room temperature at 30

min after the treatment.

The cells were transiently co-transfected with MITO_CBGN and p53_McLuc1 vectors for 24 h, which was treated with phenol red-free DMEM containing 25 mM HEPES, 0.2 mM D-luciferin, and 0.05, 0.1, 0.2 or 0.4 mM H_2O_2 (for oxidative stress) or dw (vehicle control). The luminescence intensity was measured with a microplate reader at room temperature for 4 h. As exposure to drugs, the transfected cells were treated with various concentrations of p53 inhibitors, PFT-μ (Sigma-Aldrich) or PFT-α (Millipore.Com/Calbiochem), for 1 h, and then the luminescence intensity of the cells was measured at room temperature for 2 h with or without 0.1 mM H_2O_2.

Western Blotting. HEK293T cells were lysed with RIPA buffer containing protease inhibitor cocktail, Complete EDTA-free (Roche), and centrifuged at 15,000 rpm at 4°C for 10 min. The supernatants of the cells were boiled for 5 min, which was separated by sodium dodecyl sulfate–polyacrylamide gel electrophoresis and transferred to a nitrocellulose membrane. The membrane was blocked with 5% skim milk for 1 h. Western blot analysis was performed using anti-V5 antibody (Themo Fisher Scientific-Novex), anti-DDDDK-tag pAb antibody (MEDICAL & BIOLOGICAL LABORATORIES CO., LTD.), and anti-beta-actin antibody (Sigma-Aldrich). The protein levels were measured by LAS 4000 mini (GE Healthcare).

Spectral Measurements. HEK293T cells were spread on 35-mm culture dishes and cultured in DMEM supplemented with 10% FBS and penicillin-streptomycin for 1 day under 5% CO_2 at 37°C. The cells were transiently co-transfected with the MITO_CBGN and p53_McLuc1. After 24 h of the transfection, the cells were treated

with phenol red-free DMEM containing 25 mM HEPES and 0.1 mM H_2O_2 for 1 h under 5% CO_2 at 37°C. The cells were lysed by Bright-Glo Luciferase Assay System (Promega) and transferred to 0.2 ml tubes. The tubes were placed on the sample stage of a spectrophotometer (AB-1850; ATTO), and the spectra were acquired for 10 min with a slit width of 1 mm. To measure background of the luminescence, untransfected cells of HEK293T were used. The spectral smoothing was performed by the Savitzky-Golay filtering algorithm with a window length of 41 data points.

Single Cell Imaging. HEK293T cells were plated on a poly-L-lysine-coated glass-base dish (IWAKI) and then cultured for 1 day. The cells were transiently co-transfected with MITO_CBGN and p53_McLuc1 for 1 day, and the medium was replaced with phenol red-free DMEM containing 0.2 mM D-luciferin and 1% FBS. The luminescence of the complemented luciferase was directly imaged with an inverted fluorescence and luminescence microscope (IX81; Olympus Corp.) using a 20× oil-immersion objective (0.85 NA) at room temperature (23°C). Digital images were acquired with electron multiplying charge-coupled device (EM-CCD) camera (ImagEM; Hamamatsu Photonics K.K.). Luminescence images were acquired every 10 min using 9-min exposure time; bright field (differential interference contrast) images were taken for 150 ms. After the images were acquired for 1 h, the cells were treated with 0.1 mM H_2O_2 or dw by the instillation and acquired the images for 2 h. All luminescence images were analyzed the bioluminescence intensity of single cells using the imaging software (Meta Morph; Molecular Devices Corp.) and merged with bright field images.

Statistical analysis. Paired group data were analyzed using Welch's *t*-tests after F-tests were used to evaluate whether the variances were equivalent. Data of multiple groups were analyzed one-way ANOVA. Two-series of data were analyzed by repeated measure two-way ANOVA with a multiple comparison test, Scheffe or Bonferroni/Dunn procedure.

ACKNOWLEDGEMENT

We are grateful to Dr. Rintaro Shimada of The University of Tokyo for help with the spectral smoothing. This work was supported through the Biomedical Research Unit funding scheme of the National Institute for Health Research, UK and the Japan Society for the Promotion of Science (JSPS) and the Ministry of Education, Culture, Sports, Science, and Technology (MEXT) of Japan (Grants-in-Aid for Scientific Research S 26220805 to T.O.).

CONFLICT OF INTEREST

The authors declare no conflicts of interest associated with this manuscript.

REFERENCES

Banaszynski LA, Liu CW, Wandless TJ. 2005. Characterization of the FKBP.rapamycin.FRB ternary complex. J Am Chem Soc 127(13):4715-21.

Bernardi P, Di Lisa F. 2015. The mitochondrial permeability transition pore: molecular nature and role as a target in cardioprotection. J Mol Cell Cardiol 78:100-6.

Bieging KT, Attardi LD. 2012. Deconstructing p53 transcriptional networks in tumor suppression. Trends Cell Biol 22(2):97-106.

Bieging KT, Mello SS, Attardi LD. 2014. Unravelling mechanisms of p53-mediated tumour suppression. Nat Rev Cancer 14(5):359-70.

Chipuk JE, Kuwana T, Bouchier-Hayes L, Droin NM, Newmeyer DD, Schuler M, Green DR. 2004. Direct activation of Bax by p53 mediates mitochondrial membrane permeabilization and apoptosis. Science 303(5660):1010-4.

Chow BM, Li YQ, Wong CS. 2000. Radiation-induced apoptosis in the adult central nervous system is p53-dependent. Cell Death Differ 7(8):712-20.

Dashzeveg N, Yoshida K. 2015. Cell death decision by p53 via control of the mitochondrial membrane. Cancer Lett 367(2):108-12.

Erster S, Mihara M, Kim RH, Petrenko O, Moll UM. 2004. In vivo mitochondrial p53 translocation triggers a rapid first wave of cell death in response to DNA damage that can precede p53 target gene activation. Mol Cell Biol 24(15):6728-41.

Guo X, Sesaki H, Qi X. 2014. Drp1 stabilizes p53 on the mitochondria to trigger necrosis under oxidative stress conditions in vitro and in vivo. Biochem J 461(1):137-46.

Hall MP, Unch J, Binkowski BF, Valley MP, Butler BL, Wood MG, Otto P, Zimmerman K, Vidugiris G, Machleidt T and others. 2012. Engineered luciferase reporter from a deep sea shrimp utilizing a novel imidazopyrazinone substrate. ACS Chem Biol 7(11):1848-57.

Hida N, Awais M, Takeuchi M, Ueno N, Tashiro M, Takagi C, Singh T, Hayashi M, Ohmiya Y, Ozawa T. 2009. High-sensitivity real-time imaging of dual protein-protein interactions in living subjects using multicolor luciferases. PLoS One 4(6):e5868.

Hu W, Feng Z, Teresky AK, Levine AJ. 2007. p53 regulates maternal reproduction through LIF. Nature 450(7170):721-4.

Komarov PG, Komarova EA, Kondratov RV, Christov-Tselkov K, Coon JS, Chernov MV, Gudkov AV. 1999. A chemical inhibitor of p53 that protects mice from the side effects of cancer therapy. Science 285(5434):1733-7.

Komarova EA, Chernov MV, Franks R, Wang K, Armin G, Zelnick CR, Chin DM, Bacus SS, Stark GR, Gudkov AV. 1997. Transgenic mice with p53-responsive lacZ: p53 activity varies dramatically during normal development and determines radiation and drug sensitivity in vivo. EMBO J 16(6):1391-400.

Krukowski K, Nijboer CH, Huo X, Kavelaars A, Heijnen CJ. 2015. Prevention of chemotherapy-induced peripheral neuropathy by the small-molecule inhibitor pifithrin-mu. Pain 156(11):2184-92.

Kwong JQ, Molkentin JD. 2015. Physiological and pathological roles of the mitochondrial permeability transition pore in the heart. Cell Metab 21(2):206-14.

Leu JI, Dumont P, Hafey M, Murphy ME, George DL. 2004. Mitochondrial p53 activates Bak and causes disruption of a Bak-Mcl1 complex. Nat Cell Biol 6(5):443-50.

Levine AJ, Oren M. 2009. The first 30 years of p53: growing ever more complex. Nat Rev Cancer 9(10):749-58.

Maddocks OD, Vousden KH. 2011. Metabolic regulation by p53. J Mol Med (Berl) 89(3):237-45.

Marchenko ND, Moll UM. 2014. Mitochondrial death functions of p53. Mol Cell Oncol 1(2):e955995.

Marchenko ND, Wolff S, Erster S, Becker K, Moll UM. 2007. Monoubiquitylation promotes mitochondrial p53 translocation. EMBO J 26(4):923-34.

Menendez D, Shatz M, Resnick MA. 2013. Interactions between the tumor suppressor p53 and immune responses. Curr Opin Oncol 25(1):85-92.

Millay DP, Sargent MA, Osinska H, Baines CP, Barton ER, Vuagniaux G, Sweeney HL, Robbins J, Molkentin JD. 2008. Genetic and pharmacologic inhibition of mitochondrial-dependent necrosis attenuates muscular dystrophy. Nat Med 14(4):442-7.

Mukherjee R, Mareninova OA, Odinokova IV, Huang W, Murphy J, Chvanov M, Javed MA, Wen L, Booth DM, Cane MC and others. 2016. Mechanism of mitochondrial permeability transition pore induction and damage in the pancreas: inhibition prevents acute pancreatitis by protecting production of ATP. Gut 65(8):1333-46.

Nakajima Y, Yamazaki T, Nishii S, Noguchi T, Hoshino H, Niwa K, Viviani VR, Ohmiya Y. 2010. Enhanced beetle luciferase for high-resolution bioluminescence imaging. PLoS One 5(4):e10011.

Nijboer CH, Heijnen CJ, van der Kooij MA, Zijlstra J, van Velthoven CT, Culmsee C, van Bel F, Hagberg H, Kavelaars A. 2011. Targeting the p53 pathway to protect the neonatal ischemic brain. Ann Neurol 70(2):255-64.

Ozawa T, Sako Y, Sato M, Kitamura T, Umezawa Y. 2003. A genetic approach to identifying mitochondrial proteins. Nat Biotechnol 21(3):287-93.

Ozawa T, Yoshimura H, Kim SB. 2013. Advances in fluorescence and bioluminescence imaging. Anal Chem 85(2):590-609.

Reinhardt HC, Schumacher B. 2012. The p53 network: cellular and systemic DNA damage responses in aging and cancer. Trends Genet 28(3):128-36.

Remy I, Ghaddar G, Michnick SW. 2007. Using the beta-lactamase protein-fragment complementation assay to probe dynamic protein-protein interactions. Nat Protoc 2(9):2302-6.

Roger L, Gadea G, Roux P. 2006. Control of cell migration: a tumour suppressor function for p53? Biol Cell 98(3):141-52.

Rossi F, Charlton CA, Blau HM. 1997. Monitoring protein-protein interactions in intact eukaryotic cells by beta-galactosidase complementation. Proc Natl Acad Sci U S A 94(16):8405-10.

Sablina AA, Budanov AV, Ilyinskaya GV, Agapova LS, Kravchenko JE, Chumakov PM. 2005. The antioxidant function of the p53 tumor suppressor. Nat Med 11(12):1306-13.

Shimomura O. 2012. The Fireflies and Luminous Insects. Bioluminescence : chemical principles and methods. Rev. ed. New Jersey: World Scientific. p 1-30.

Song S, Lambert PF. 1999. Different responses of epidermal and hair follicular cells to radiation correlate with distinct patterns of p53 and p21 induction. Am J Pathol 155(4):1121-7.

Strom E, Sathe S, Komarov PG, Chernova OB, Pavlovska I, Shyshynova I, Bosykh DA, Burdelya LG, Macklis RM, Skaliter R and others. 2006. Small-molecule inhibitor of p53 binding to mitochondria protects mice from gamma radiation. Nat Chem Biol 2(9):474-9.

Tedeschi A, Di Giovanni S. 2009. The non-apoptotic role of p53 in neuronal biology: enlightening the dark side of the moon. EMBO Rep 10(6):576-83.

Teodoro JG, Parker AE, Zhu X, Green MR. 2006. p53-mediated inhibition of angiogenesis through up-regulation of a collagen prolyl hydroxylase. Science 313(5789):968-71.

Vaseva AV, Marchenko ND, Ji K, Tsirka SE, Holzmann S, Moll UM. 2012. p53 opens the mitochondrial permeability transition pore to trigger necrosis. Cell 149(7):1536-48.

Villalobos V, Naik S, Bruinsma M, Dothager RS, Pan MH, Samrakandi M, Moss B, Elhammali A, Piwnica-Worms D. 2010. Dual-color click beetle luciferase heteroprotein fragment complementation assays. Chem Biol 17(9):1018-29.

Viviani VR, Silva AC, Perez GL, Santelli RV, Bechara EJ, Reinach FC. 1999. Cloning and molecular characterization of the cDNA for the Brazilian larval click-beetle Pyrearinus termitilluminans luciferase. Photochem Photobiol 70(2):254-60.

Vogelstein B, Lane D, Levine AJ. 2000. Surfing the p53 network. Nature 408(6810):307-10.

Wehr MC, Rossner MJ. 2016. Split protein biosensor assays in molecular pharmacological studies. Drug Discov Today 21(3):415-29.

Zhang L, Yu D, Hu M, Xiong S, Lang A, Ellis LM, Pollock RE. 2000. Wild-type p53 suppresses angiogenesis in human leiomyosarcoma and synovial sarcoma by transcriptional suppression of vascular endothelial growth factor expression. Cancer Res 60(13):3655-61.

Zhao Y, Chaiswing L, Velez JM, Batinic-Haberle I, Colburn NH, Oberley TD, St Clair DK. 2005. p53 translocation to mitochondria precedes its nuclear translocation

and targets mitochondrial oxidative defense protein-manganese superoxide dismutase. Cancer Res 65(9):3745-50.

FIGURE LEGENDS

Figure 1. Schematic of luciferase fragment complementation assays based on the FKBP-FRB interactions. Rapamycin induces binding of FKBP to FRB, which causes the complementation of CBGN and McLuc1, resulting in the restoration of the luminescence. V5/His indicates an epitope tag (V5) and a tag composed of six histidine residues (His), respectively.

Figure 2. Comparison of luminescence intensity of rapamycin-induced luciferase complementation. HEK293T cells were spread on a 96-well microtiter plate and transiently co-transfected with ELucN_FKBP and FRB_McLuc1, or CBGN_FKBP and FRB_McLuc1, respectively, for 2 days under 5% CO_2 at 37°C. The medium was replaced with phenol red-free DMEM containing 25 mM HEPES, 1 μM rapamycin or DMSO, as a vehicle control, and 0.2 mM D-luciferin. The luminescence was measured with a microplate reader at 30 min after the treatment. Data were expressed as mean ± SD (n=5). **: $p < 0.01$.

Figure 3. Schematic of luciferase fragment complementation assays via p53 translocation into mitochondrial matrix. (a) Schematic diagrams of the constructs, MITO_CBGN, p53_McLuc1, and MITO_CBG, to evaluate p53 translocation into mitochondria. MITO_CBG vector was constructed to confirm whether H_2O_2 interfered with the luciferin-luciferase reaction. These vectors are driven by cytomegalovirus promoter. MITO indicates a mitochondrial matrix targeting signal. (b) When the cells transfected with p53_McLuc1 and MITO_CBGN are stimulated with H_2O_2, p53_McLuc1 translocates into mitochondrial matrix, where McLuc1 complements with mitochondrial localized CBGN and results in bioluminescence. FLAG and V5/His

indicate epitope tags (FLAG and V5) and a tag composed of six histidine residues (His), respectively.

Figure 4. Luminescence intensity of CBGN-McLuc1 complementation depending on p53 translocation into mitochondrial matrix by H_2O_2. (a-c) HEK293T cells were transiently transfected with p53_McLuc1 and MITO_CBGN (a, c) or MITO_CBG (b), respectively, for 24 h under 5% CO_2 at 37°C, the medium of which was replaced with phenol red-free DMEM containing 25 mM HEPES, 0.05, 0.1, 0.2, or 0.4 mM H_2O_2 or dw, as a vehicle control, and 0.2 mM D-luciferin. (a, b) The luminescence intensity of the cells was measured with a microplate reader for 4 h. Data were expressed as mean ± SD (n=5). (a, right) Bar graph indicates the light intensity of H_2O_2-treated cells expressing p53_McLuc1 and MITO_CBGN at 120 min in the left graph. **: $p < 0.01$ vs. respective vehicle. ++: $p < 0.01$. (c) The amount of protein was analyzed by Western blotting at 120 min after H_2O_2 treatment. '-' and 'veh' indicate untransfected cells and vehicle control, respectively (a-c).

Figure 5. Decrease in luminescence intensity based on inhibition of p53 translocation from cytosol into mitochondrial matrix by PFT-μ. (a-c) HEK293T cells were transiently transfected with p53_McLuc1 and MITO_CBGN (a, c) or MITO_CBG (b), respectively, for 24 h under 5% CO_2 at 37°C, the medium of which was replaced with phenol red-free DMEM containing 25 mM HEPES and 10, 20, or 40 μM PFT-μ or DMSO (vehicle control) for 1 h. The medium of the cells was exchanged with phenol red-free DMEM containing 0.1 mM H_2O_2 or dw (vehicle control) and 0.2 mM D-luciferin. (a, b) The luminescence intensity of the cells was measured with a microplate reader for 2 h. Data were expressed as mean ± SD (n = 6; untransfected cells,

n = 4). (a, right) Bar graph indicates the light intensity of H_2O_2-treated cells with or without PFT-μ expressing p53_McLuc1 and MITO_CBGN at 120 min in the left graph. **: $p < 0.01$ vs. respective vehicle under 0.1 mM H_2O_2 treatment. ++: $p < 0.01$. (c) The amount of protein was analyzed by Western blotting at 90 min after H_2O_2 treatment. '-' and 'veh' indicate untransfected cells and vehicle control, respectively (a, c).

Figure 6. Luminescence intensity based on p53 translocation into mitochondrial matrix using PFT-α-treated cells. (a, b) HEK293T cells were transiently transfected with p53_McLuc1 and MITO_CBGN (a) or MITO_CBG (b), respectively, for 24 h under 5% CO_2 at 37°C, the medium of which was replaced with phenol red-free DMEM containing 25 mM HEPES and 5, 10, or 20 μM PFT-α or DMSO (vehicle control) for 1 h. The medium of the cells was exchanged with phenol red-free DMEM containing 0.1 mM H_2O_2 or dw, as a vehicle control, and 0.2 mM D-luciferin, and the luminescence intensity of the cells was measured with a microplate reader for 2 h. Data were expressed as mean ± SD (n=5). (a, right) Bar graph indicates the light intensity of H_2O_2-treated cells with or without PFT-α expressing p53_McLuc1 and MITO_CBGN at 120 min in the left graph. '-' indicates untransfected cells.

Figure 7. Emission spectrum of the luciferase based on CBGN-McLuc1 complementation. HEK293T cells were transiently co-transfected with p53_McLuc1 and MITO_CBGN for 24 h. The medium of the cells was replaced with phenol red-free DMEM containing 25 mM HEPES and 0.1 mM H_2O_2 and then incubated for 1 h under 5% CO_2 at 37°C. The cells were lysed with a reagent containing luciferin, and the luminescence spectrum was measured using a spectrophotometer. The data smoothing was performed by the Savitzky-Golay (S-G) filtering algorithm (green line). The

magenta line indicates the raw data of the luminescence spectrum based on CBGN-McLuc1 complementation.

Figure 8. Time-lapse bioluminescence imaging of CBGN-McLuc1 complementation depending on p53 translocation into the mitochondrial matrix by H_2O_2 treatment at a single cell level. (a, b) HEK293T cells were plated on a glass-base dish and then cultured for 1 day. The cells were transiently co-transfected with p53_McLuc1 and MITO_CBGN for 24 h, and the medium was replaced with phenol red-free DMEM containing 0.2 mM D-luciferin and 1% FBS. After the bioluminescence imaging was acquired at a single cell level for 1 h, the cells were treated with 0.1 mM H_2O_2 or dw and then acquired the images for 2 h. The imaging data was obtained every 10 min using 9-min exposure time. Time 0 indicates the initiation of the time-lapse bioluminescence imaging. Arrow represents the initiation of H_2O_2 treatment. (a) The light intensity of individual cells was shown as the relative value. (b) The light intensity of three individual cells was shown as mean ± SD. **: $p < 0.01$ vs. respective vehicle control.

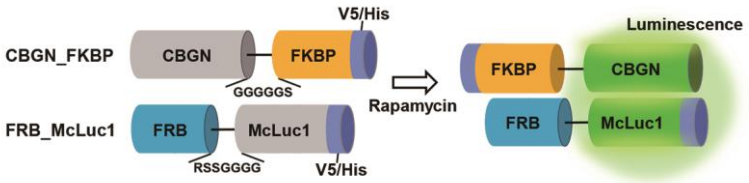

Fig. 1.

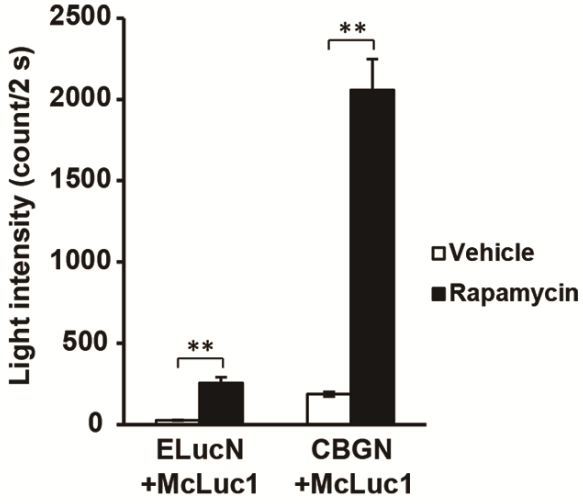

Fig. 2.

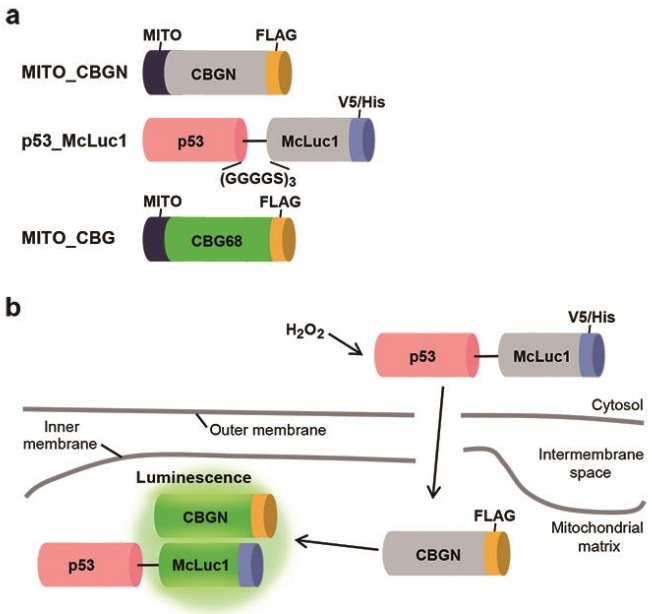

Fig. 3.

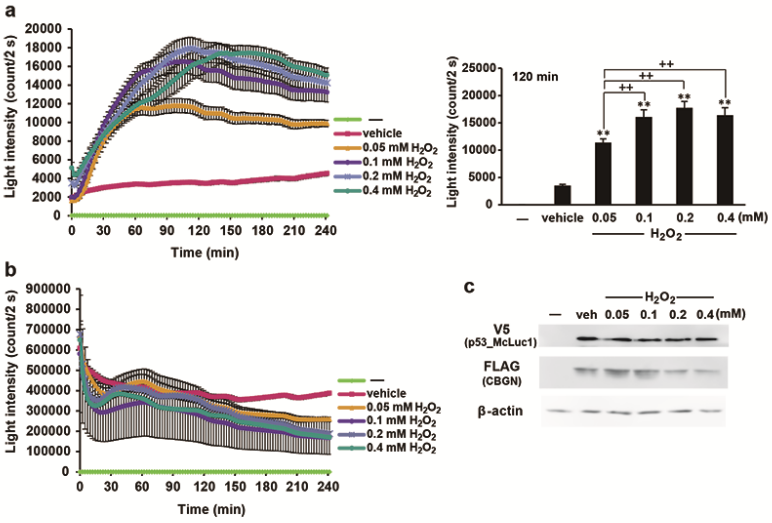

Fig. 4.

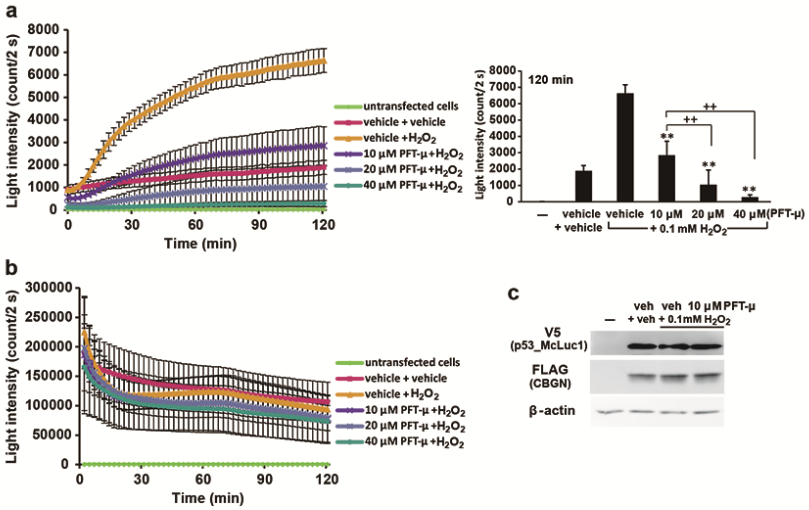

Fig. 5.

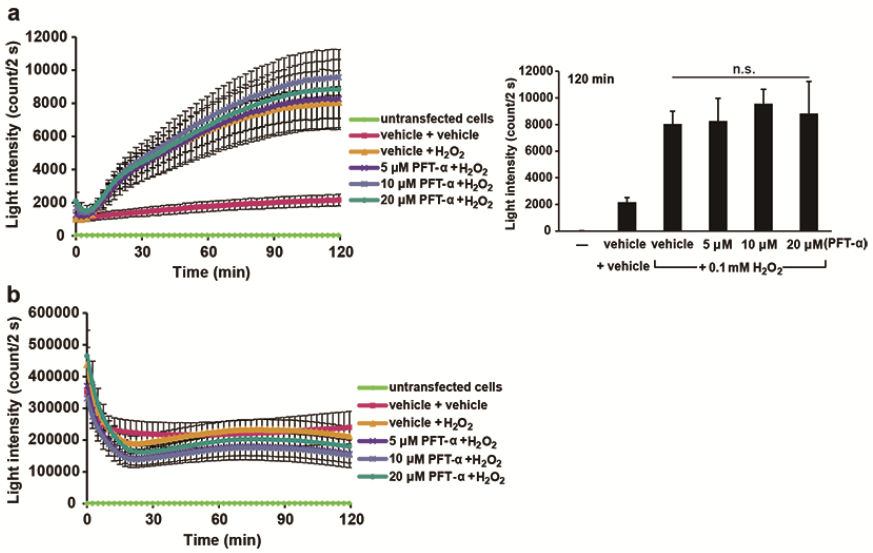

Fig. 6.

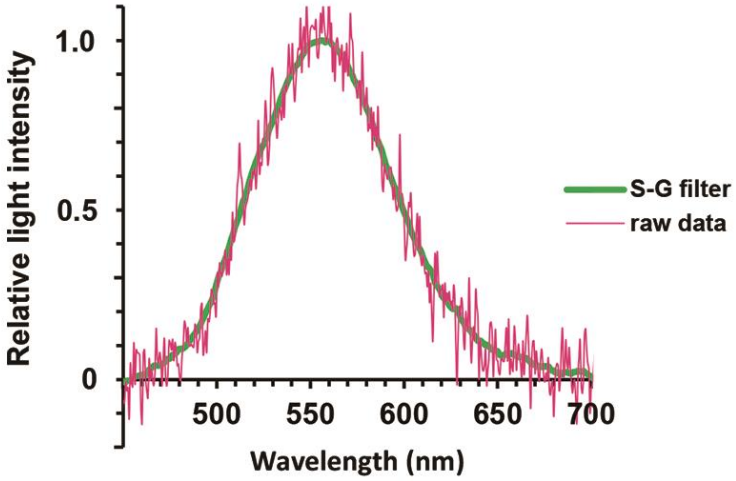

Fig. 7.

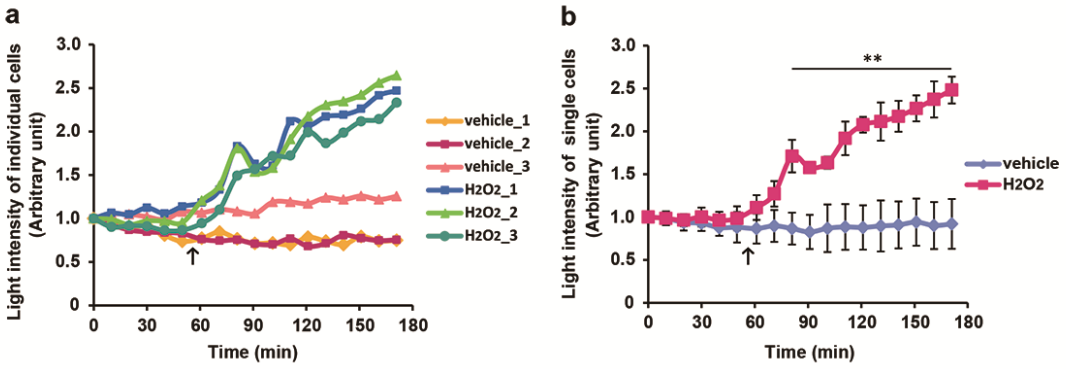

Fig. 8.